

Electronic Supplementary Information

for

“Dual anti-angiogenic and cytotoxic properties of ruthenium(III) complexes containing pyrazolato and/or pyrazole ligands”

Raymond Wai-Yin Sun,¹ Miro Fei-Yeung Ng,¹ Ella Lai-Ming Wong,¹ Jingfei Zhang,¹ Stephen Sin-Yin Chui,¹ Lam Shek,² Tai-Chu Lau,^{*2} and Chi-Ming Che^{*1}

¹*Department of Chemistry and Open Laboratory of Chemical Biology of the Institute of Molecular Technology for Drug Discovery and Synthesis, The University of Hong Kong, Pokfulam Road, Hong Kong, China, and* ²*Department of Biology and Chemistry, City University of Hong Kong, Tat Chee Avenue, Kowloon Tong, Hong Kong, China.*

Fax: (+852) 2857-1586; E-mail: cmche@hku.hk, bhtclau@cityu.edu.hk

Part I. Experimental Section

Materials. All chemicals, except otherwise noted, were purchased from Sigma-Aldrich Chemical Co. Ru₂(OAc)₄Cl was prepared according to literature method [R. W. Mitchell, A. Spencer, G. Wilkinson, *J. Chem. Soc., Dalton Trans.*, **1973**, 846]. Acetonitrile and dichloromethane were freshly distilled from CaH₂. Analytical-grade organic solvents and double-distilled deionized water were used throughout the experiments.

Cell Proliferation Kit I (MTT) and Propidium Iodide Staining Kit were purchased from Roche. Nitric oxide (NO) Assay kit was purchased from Stressgen. Cell culture dishes and 96-well microtitre plates were purchased from Nalge Nunc Int. Phosphate-buffered saline (PBS) was obtained from Gibco BRL.

Instrumentation. All absorption spectra were recorded on a PerkinElmer Lambda 900 UV/VIS/NIR spectrophotometer. Positive ion fast atom bombardment (FAB) mass spectra were recorded on a Finnigan MAT95 mass spectrometer using 3-nitrobenzyl alcohol as matrix. Electrospray ionization (ESI) mass spectra were recorded on a Finnigan LCQ mass spectrometer. Cyclic voltammetry was recorded by using a PAR Potentiostat/Galvanostat Model 273A. Absorption of the MTT and the nitric oxide assays was determined by using a MR700 microtitre plate reader (Molecular Devices). Flow cytometric analysis was performed with a Coulter EPICS flow cytometer equipped with 480 nm long pass, 525 nm band pass and 625 nm long pass mirrors. Fluorescent signals were excited by 15 mW air-cool argon convergent laser at 488 nm. Fluorescent signals were manipulated with Coulter Elite 4.0 software and were analyzed by Winlist 1.04 and Modfit 5.11 software (Verity Software House). Ruthenium-content analysis was undertaken using Agilent 7500 inductively-coupled plasma-mass spectrometer (ICP-MS).

Synthesis.

$Ru_2(\mu_2-O)(\mu_2-pz)_2(pz)_2(pzH)_4$ (**1**)

The ruthenium(III) complex (**1**) was prepared by the reaction of $Ru_2(OAc)_4Cl$ (500 mg, 1.055 mmol) with an excess of pyrazole (pz, 681 mg, 10 mmol) in a MeOH-H₂O (1:1, v/v) solution (20 mL) at room temperature. Heating was not required but agitation was preferred. The color of the solution changed from orange-red to purple within 3 minutes, and a deep-blue color was eventually obtained. The solution was evaporated to dryness and the solid was re-dissolved in CH₂Cl₂ (2 × 2 mL). Hexane (30 mL) was added to the filtrate, and the deep blue powder was filtered and washed with hexane. Yield: 88%. UV/Vis (CH₂Cl₂) λ_{max}/nm (log ϵ): 260 (15,000), 408 (sh, 2,000), 589 (9,100). FAB-MS (+ve, m/z): 760 [$Ru_2(pz)_8O \cdot H_5$]⁺, 692 [$Ru_2(pz)_7O \cdot H_4$]⁺, 624 [$Ru_2(pz)_6O \cdot H_3$]⁺, 556 [$Ru_2(pz)_5O \cdot H_2$]⁺, 488 [$Ru_2(pz)_4O \cdot H$]⁺, 420 [$Ru_2(pz)_3O$]⁺. ESI-MS (+ve, m/z): 760 [$Ru_2(pz)_8O \cdot H_5$]⁺. Anal. Calcd. for C₂₄H₂₆N₁₆Ru₂·H₂O: C, 37.99%; H, 3.72%, N, 29.54%; Found: C, 37.81; H, 4.01, N, 29.43%.

trans-[$Ru^{III}(pzH)_4(Cl)_2$]Cl (**2**)

This compound was synthesized by a procedure that is different from the literature method. $RuCl_3 \cdot xH_2O$ (144 mg, 0.584 mmol) was dissolved in 2-methoxyethanol (15 mL) and 10 equivalents of pyrazole (398 mg, 5.85 mmol) was added. The mixture was refluxed for 24 h. Diethyl ether was added to the dark brown solution, and the resulting brown precipitate was filtered and washed with diethyl ether. Yield: 82 mg (29 %). Anal. Calcd for $RuCl_{12}H_{16}N_8Cl_3$ (M.W. 479.73): C 30.04, H 3.36, N 23.36. Found: C 29.86, H 3.48, N 23.26. UV/Vis (CH₃OH), λ_{max} , nm (ϵ , M⁻¹ cm⁻¹): 408(3200), 354(2500), 229(15000), 205(18700). IR (cm⁻¹, KBr): $\nu(N-H)$ 3202 (s), $\nu(C=N)$ 1470 (s). ESI-MS: $m/z = 444$ (M⁺), $m/z = 376$ (M⁺ - pz), $m/z = 308$ (M⁺ - 2 pz).

trans-[$Ru^{III}(3(5)-mepzH)_4(Cl)_2$]Cl (**3**)

[(DMSO)₂H]*trans*-[$Ru^{III}(DMSO)_2(Cl)_4$] (100 mg, 0.18 mmol) was dissolved in 3-methylpyrazole (1 mL). The mixture was heated at 130 °C and stirred for 1 h. The dark brown solution was cooled down and the resulting orange-red precipitate was filtered and then washed with diethyl ether. The compound was recrystallized by diffusion of diethyl ether into a methanol solution of the complex. Yield: 30 mg (31 %). Anal. Calcd for $RuCl_{16}H_{24}N_8Cl_3$ (M.W. 535.83): C 35.86, H 4.51, N 20.91. Found: C 35.96, H 4.31, N 20.80. UV/Vis (CH₃OH), λ_{max} , nm (ϵ , M⁻¹ cm⁻¹): 437(5500), 350(2300), 369(5600), 234(18400), 203(23500). IR (cm⁻¹, KBr): $\nu(N-H)$ 3170 (s), $\nu(C=N)$ 1564 (s). ESI-MS: $m/z = 500$ (M⁺), $m/z = 418$ (M⁺ - 3(5)mepz), $m/z = 336$ (M⁺ - 2 3(5)mepz).

[$Ru^{II}(3(5)-mepzH)_6$](Cl)₂ (**4**)

cis-[$Ru^{II}(DMSO)_4(Cl)_2$] (90 mg, 0.186 mmol) was dissolved in 3-methylpyrazole (1.4 mL). The mixture was heated to 130 °C and stirred for 30 min. Diethyl ether was added to the resulting dark brown solution and the pale brown precipitate was filtered

and washed with diethyl ether. The compound was re-crystallized by diffusion of diethyl ether into a methanol solution of the complex. Yield: 46 mg (37 %). Anal. Calcd for $\text{RuC}_{24}\text{H}_{36}\text{N}_{12}\text{Cl}_2$ (M.W. 664.62): C 43.37, H 5.46, N 25.29. Found: C 43.06, H 5.61, N 25.36. UV/Vis (CH_3OH), λ_{max} , nm (ϵ , $\text{M}^{-1} \text{cm}^{-1}$): 279(20100), 206(27900). IR (cm^{-1} , KBr): $\nu(\text{N-H})$ 3178 (s), $\nu(\text{C=N})$ 1578 (s). ESI-MS: $m/z = 593$ ($\text{M}^+ - \text{H} - \text{Cl}$). $^1\text{H NMR}$ (D_2O ; δ): 2.07 (s, 18H); 6.05 (d, 6H); 7.23 (d, 6H).

cis- $[\text{Ru}^{\text{II}}(\text{BiIml})_2(\text{DMSO})_2](\text{ClO}_4)_2$ (**5**)

$[(\text{DMSO})_2\text{H}]\text{trans}$ - $[\text{Ru}^{\text{III}}(\text{DMSO})_2\text{Cl}_4]$ and 2,2'-bi-2-imidazoline were prepared by literature methods [E. Alessio, G. Balducci, M. Calligaris, G. Costa, W. M. Attia, G. Mestroni, *Inorg. Chem.* **1991**, *30*, 609; J. C. Wang, J. E. Bauman, *Inorg. Chem.* **1965**, *4*, 1613]. A mixture of $[(\text{DMSO})_2\text{H}]\text{trans}$ - $[\text{Ru}^{\text{III}}(\text{DMSO})_2\text{Cl}_4]$ (95 mg, 0.17 mmol) and 2,2'-bi-2-imidazoline (71 mg, 0.51 mmol) in ethanol (10 mL) was refluxed for 16 h. The solution was filtered and saturated NaClO_4 solution (1 mL) was added to the reddish brown filtrate. The resulting yellow precipitate was filtered and washed with diethyl ether. The product was recrystallized from water. Crystals suitable for X-ray crystallography were grown by slow evaporation of a DMF solution of the complex. Yield: 73 mg (59 %). Anal. Calcd for $\text{RuC}_{16}\text{H}_{32}\text{N}_8\text{O}_{10}\text{Cl}_2\text{S}_2$ (M.W. 732.6): C 26.23, H 4.41, N 15.29. Found: C 25.87, H 4.24, N 15.23. IR (cm^{-1} , KBr): $\nu_{\text{N-H}}$ 3329 (s), $\nu_{\text{C=N}}$ 1567 (vs). ESI-MS: $m/z = 633$ (M^+), $m/z = 555$ ($\text{M}^+ - \text{DMSO}$). $^1\text{H NMR}$ (CD_3OD ; δ): 2.65, 2.91 (s, 6H each, CH_3S); 4.01 (m, 16H, $\text{CH}_2\text{-BiIml}$).

Warning: *Perchlorate salts are potentially explosive. Although no explosions have been experienced in this preparation, the amount of ruthenium complex prepared should be less than 100 mg each time.*

X-Ray crystal determination. Crystals of **1** were obtained by slow evaporation of a CH_2Cl_2 -hexane (1:2, v/v) solution. A purple bar-shaped crystal of dimension $0.10 \times 0.03 \times 0.03 \text{ mm}^3$ was mounted on a glass capillary tube and subjected to X-ray diffraction at $-173 \text{ }^\circ\text{C}$ on a BRUKER X8 PROTEUM diffractometer with a CCD detector using micro-focus rotating anode X-ray generator Cu- K_α radiation ($\lambda = 1.5418 \text{ \AA}$). Data collection was made with a 0.5° oscillation step of all angles, 5 seconds exposure time and a detector distance at 60 mm. The collected images were interpreted and intensities integrated and scaled using PROTEUM2 program [PROTEUM2 v2009.3-0, 2003, 2004 Bruker Nonius, 2005-2009 Bruker AXS]. The structure was solved by direct method employing SHELXS-97 program on a PC. The two ruthenium atoms were firstly located and the positions of other non-hydrogen atoms were found after few cycles of refinement based on the full-matrix least-squares using SHELXL-97 program. In the final stage of refinement, the Fourier difference map analysis clearly reveals four electron peaks ($0.6\text{--}0.8 \text{ e}\text{\AA}^3$) that were located at $0.6\text{--}1.0 \text{ \AA}$ near the uncoordinated N atoms (N3B, N5B, N7B, N8B) of the non-bridging pyrazolate ligands, which reasonably account for the formation of intra- and intermolecular hydrogen bonds. On the contrary, there is no apparent peak ($> 0.3 \text{ e}\text{\AA}^3$) in a close proximity to the O1 atom of the oxo-bridge and the N4B and N6B atoms of the non-bridging pyrazolate ligands. Based on this X-ray data and diamagnetic nature of this complex, the entitled formulation of

this Ru₂ complex is confirmed, based on one unit of an oxo-bridged dimeric Ru(III) core with four pyrazolate mono-anions (two are bridging and two are non-bridging) and four neutral pyrazole ligands.

Electrochemical measurements. Electrochemical potentials of the ruthenium complexes were measured by cyclic voltammetry. Electrochemical measurements were performed at room temperature under a nitrogen atmosphere using 0.1 M tetrabutylammonium hexafluorophosphate/ DMF as supporting electrolyte. The working electrode was a glassy carbon (Atomergic Chemetal V25, geometric area of 0.35 cm²) electrode and the counter electrode was platinum wire. A non-aqueous Ag/AgNO₃ (0.1 M in DMF) reference electrode was contained in a separate compartment connected to the test solution via fine sintered glass disks. The ferrocenium/ferrocene couple was used as the internal standard.

Stability analysis. Solution stability of **1** was examined by UV/Vis spectrophotometer. The absorption spectra of **1** in a PBS-EtOH (19:1, v/v) solution in the presence or absence of ascorbic acid (0.1 mM) were monitored for 72 h at room temperature.

Cell lines and cell cultures. Human cervical epithelioid carcinoma cells (HeLa), hepatocellular carcinoma cells (HepG2) and normal lung fibroblast cells (CCD-19Lu) and normal mouse pancreatic islet endothelial cells (MS1) were obtained commercially from American Type Culture Collection (ATCC). Human nasopharyngeal carcinoma cells (SUNE1) were derived from poorly differentiated NPC in Chinese patients, and were generously provided by Prof. S. W. Tsao (Department of Anatomy, The University of Hong Kong, Hong Kong). HeLa and CCD-19Lu were maintained in a minimum essential medium (MEM) with Earle's balanced salts supplemented with non-essential amino acids (0.1 mM). SUNE1 cells were maintained in the RPMI 1640 medium. HepG2 and MS1 cells were maintained in Dulbecco's modified Eagle's medium (DMEM) with high glucose content. All media were supplemented with fetal bovine serum (10%) and L-glutamine (2 mM). Penicillin (100 U/mL) and streptomycin (100 μg/mL) were added to all media. Cultures were incubated at 37 °C in a 5% CO₂/95% air humidified atmosphere and were sub-cultured when 90% confluence was reached.

Cytotoxicity evaluation. Cells were seeded at a density of 1 × 10⁴ cells/ well in 96-well flat-bottomed microtitre plates with supplemented cultured medium (100 μL/ well) 24 h before the drug treatment. Complexes **1 - 5** and cisplatin (positive control) were dissolved in the culture medium. Each complex was added to each well with serial dilution and the plates were incubated at 37 °C in a 5% CO₂/95% air for 72 h. By means of the 3-(4,5-dimethylthiazol-2-yl)-2,5-diphenyltetrazolium bromide (MTT) assay [T. Mosmann, *J. Immunol. Methods*, 1983, **65**, 55], MTT solution (10 μL, 5 mg/mL in PBS) was added to each well, and the plates were incubated for another 4 h. Solubilization buffer (100 μL, 10%SDS in 0.01 M HCl) was added into each well. The plates were left incubated overnight. Absorbance at 550 nm was measured by a microtitre plate reader. The IC₅₀ values of

the complexes were evaluated based on the percentage of cell survival in a dose-dependent manner relative to the negative untreated control.

Cell-cycle analysis. HeLa cells were seeded at a density of 1×10^6 cells/dish in 60 mm-culture dishes and incubated at 37 °C in a 5% CO₂/95% air for 24 h. After 24 or 48 h incubation, cells treated with **1** (10 μM) or vehicle control were harvested, trypsinized, washed twice with cold PBS and fixed in 70% ethanol. Cells were rehydrated in PBS and stained in a propidium iodide (50 μg/mL) solution containing RNase A (5 U/mL) for 30 min. Cells (3×10^4) from each sample were counted in the flow cytometry. The data was analyzed using Modfit 5.11 software.

DNA absorption titration. A solution of **1** (50 μM) in PBS/EtOH (19:1, v/v, 3000 μL) was placed in a thermostated cuvette in a UV/Vis spectrophotometer, and the absorption spectrum was recorded. Aliquots of a millimolar stock calf-thymus DNA (ctDNA) solution were added to the solution of **1** and absorption spectra were recorded. The binding constant for **1** toward ctDNA was determined by the Scatchard equation (C. V. Kumra, E. H. Asuncion, *J. Am. Chem. Soc.* **1993**, *115*, 8547).

Gel-mobility-shift assay. A 100-bp PCR product (15.2 μM bp⁻¹) was mixed with ethidium bromide (EB), Hoechst 33342 (H33342), or **1** (5 and 50 μM). The mixtures were analyzed by gel electrophoresis using a 2% (w/v) agarose gel and tris-acetate-EDTA (TAE) buffer. The gel was stained by immersion into a bath of EB after electrophoresis and was visualized under UV illumination.

Topoisomerase I inhibition assay. Plasmid DNA (2.9 kb) was purchased from Promega (Madison, WI, USA) at a concentration of 1 μg/mL. It was diluted to the working concentration in reaction buffer (50 mM Tris/HCl (pH 7.5), 20 mM KCl, 1 mM EDTA, 0.3 mg/mL BSA and 1 mM dithiothreitol). Recombinant topoisomerase I (topo I) was kindly provided by Prof. Y. C. Cheng (Pharmacology, Yale University). Supercoiled (SC) plasmid DNA was diluted by using reaction buffer to a concentration of 25 ng/μL. To a 75 ng of SC DNA dilution, aliquot of **1** (1 μL) dissolved in PBS-EtOH (19:1, v/v), CPT or vehicle control was added. The mixtures were incubated for 20 min at room temperature and topo I solution (2 μL) was added. This solution was incubated at 37 °C for 2 h. The reaction was terminated by addition of a 20% sodium dodecyl sulfate (SDS, 1.25 μL) solution and proteinase K (2.5 μL, 1 mg/mL). After incubation at 45 °C for 1 h, the samples were analyzed by gel electrophoresis using 1% (w/v) agarose gels containing 0.1% (w/v) SDS. The gel was stained by immersion into a bath of EB after electrophoresis and was visualized under UV illumination.

Detection of reactive oxygen species (ROS). Stock solution (10 mM) of rhodamine-123 (DHRh-123) was prepared in DMSO and purged with argon prior to storage in dark at -80°C . HeLa cells were seeded at 6000 cells/well in a 96-well black-bottomed plate for 24 h prior to sample addition. Cells were then washed once with Hank's balanced salt solution (HBSS) and were incubated in the presence of **1** with DHRh-123 ($5\ \mu\text{M}$) for 0 to 5 h. At the end of each incubation, the cells were washed twice with HBSS. Fluorescent signal at 530 nm was quantified with excitation at 485 nm.

Nitric Oxide Assay. MS1 cells were cultured on 24-well plates at a density of 1×10^4 cells/well. After 24 h, the medium was replaced by supplemented DMEM containing lipopolysaccharide (LPS, $10\ \mu\text{M}$) and the ruthenium complexes (**1-5**, $10\ \mu\text{M}$). Culture supernatants were collected after 24 h of incubation. NO production was assessed by measuring the concentration of nitrate, a stable degradation product of NO, with the Griess reagents.

Tube-formation assay. By using the *In Vitro* Angiogenesis Kit, $10\times$ Diluent Buffer and ECMatrixTM solution were mixed in a ratio of 1:9. The mixture ($50\ \mu\text{L}$) was transferred to each well of a 96-well plate. The matrix solution was incubated at $37\ ^{\circ}\text{C}$ to allow polymerization. After 1h, MS1 cells (50,000) premixed with different concentrations of **1 - 5** (0, 1.25, 2.5, $5\ \mu\text{M}$) in $100\ \mu\text{L}$ of DMEM medium were added to the top of the polymerized matrix. After incubation at $37\ ^{\circ}\text{C}$ for 8 h, tube formation was examined under an inverted light microscope at $100\times$ magnification and was quantified using the Sigma Scan Pro. software. The percentage of inhibition was calculated based on the distance measured relative to the untreated control.

Wound-healing assay. MS1 cells were cultured on 60-mm culture dishes at a density of 2×10^6 cells/dish. After 24 h, a single wound was created in the middle of the cell monolayer by gently removing the attached cells with a sterile plastic pipette tip. The cells were washed twice with PBS and solutions of different concentrations of **1** (0, 1.25, 2.5, $5\ \mu\text{M}$) in 5 mL of DMEM were added. After incubation at $37\ ^{\circ}\text{C}$ for 8 h, migration of the cells into the wound was observed under an inverted microscope.

Cellular-uptake experiment. Cellular uptake experiments were conducted according to the literature method with some modifications (M. J. McKeage, S. J. Berners-Price, P. Galettis, R. J. Bowen, W. Brouwer, D. Li, Z. Li, B. B. Baguley, *Cancer Chemother. Pharmacol.* **2000**, *46*, 343). HeLa cells were seeded at a density of 1×10^6 cells/dish in 6-cm culture dishes. After 24 h, cells in different culture dishes were separately treated with **1** ($10\ \mu\text{M}$), **2** ($10\ \mu\text{M}$), **3** ($10\ \mu\text{M}$) or vehicle control. Cells were harvested after 4 h, trypsinized and washed four times with ice-cold PBS. Milli-Q water ($500\ \mu\text{L}$) was added and monolayered cells were scraped off from the culture dishes. All samples ($300\ \mu\text{L}$) were digested in 70% HNO_3 ($500\ \mu\text{L}$) at $70\ ^{\circ}\text{C}$ for 2 h, which were then diluted by water (sample: water, 1:100) for ICP-MS analysis.

Part II. Figures and Tables

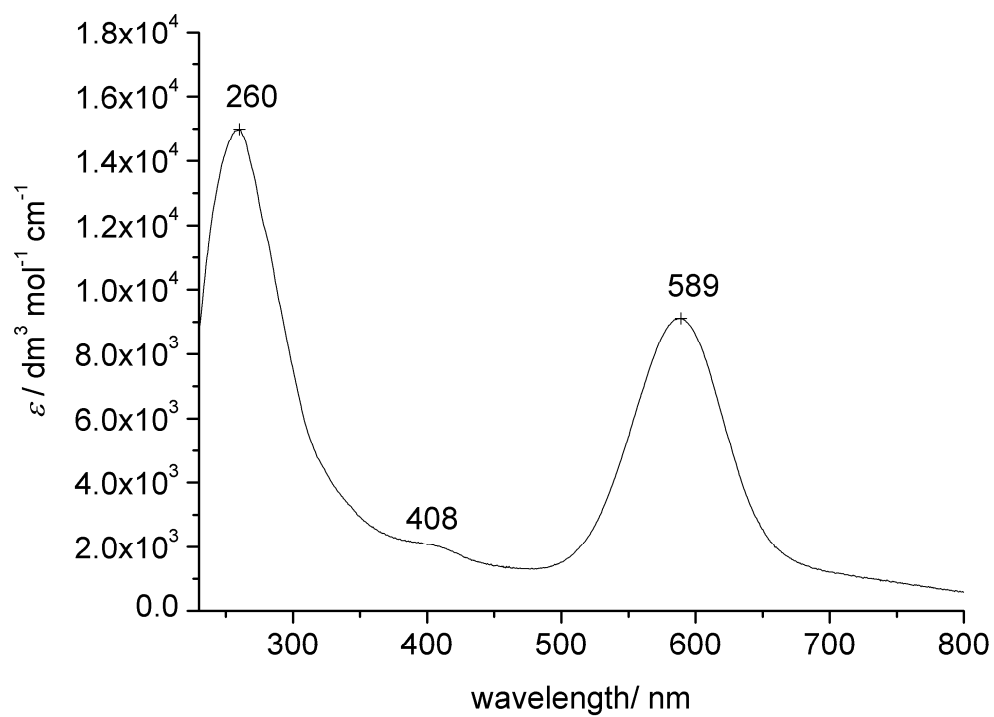


Figure S1. UV/Vis absorption spectrum of **1** in CH₂Cl₂

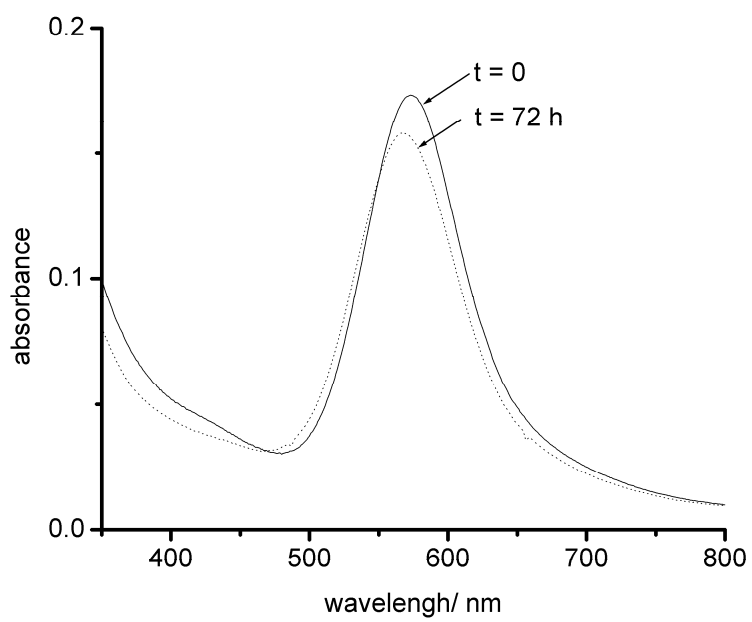


Figure S2. UV/Vis spectra of **1** in a PBS-EtOH solution (19:1, v/v) at time = 0 and 72 h.

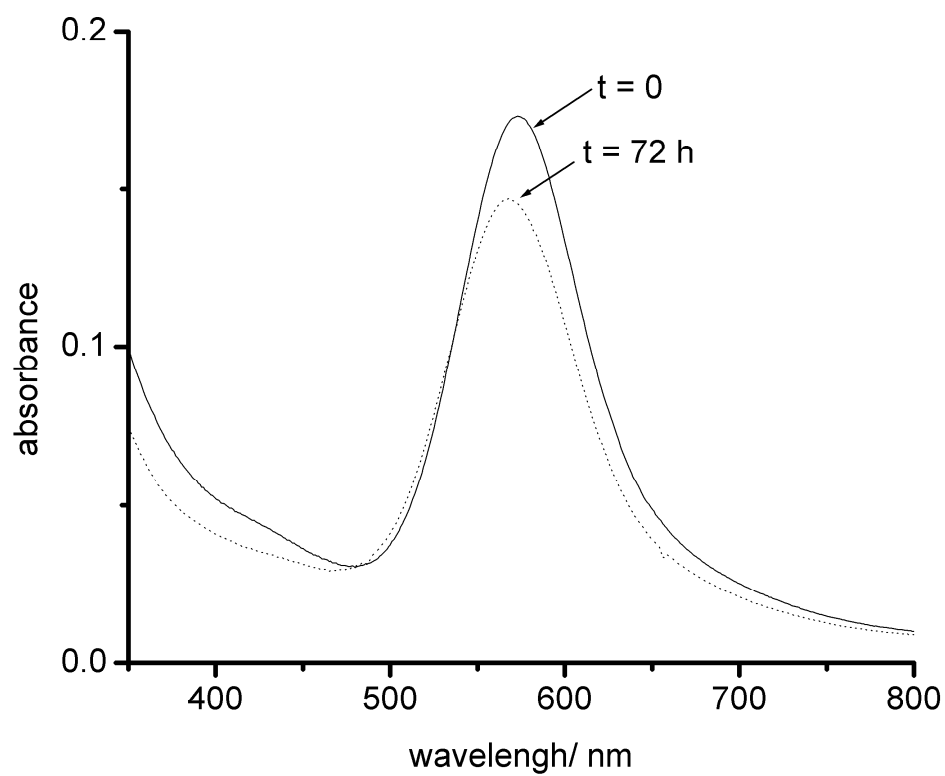


Figure S3. UV/Vis spectra of **1** in a PBS-EtOH solution (19:1, v/v) containing ascorbic acid (0.1 mM) at time = 0 and 72 h.

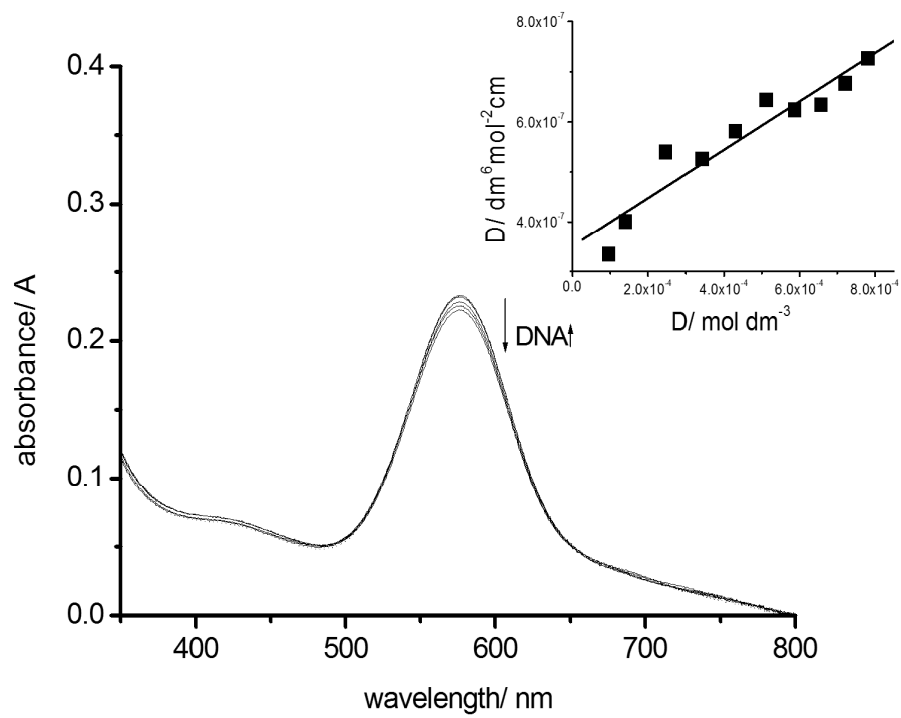


Figure S4. UV/Vis spectral changes of **1** in a PBS-EtOH solution (19:1, v/v) with increasing concentration of calf-thymus DNA.

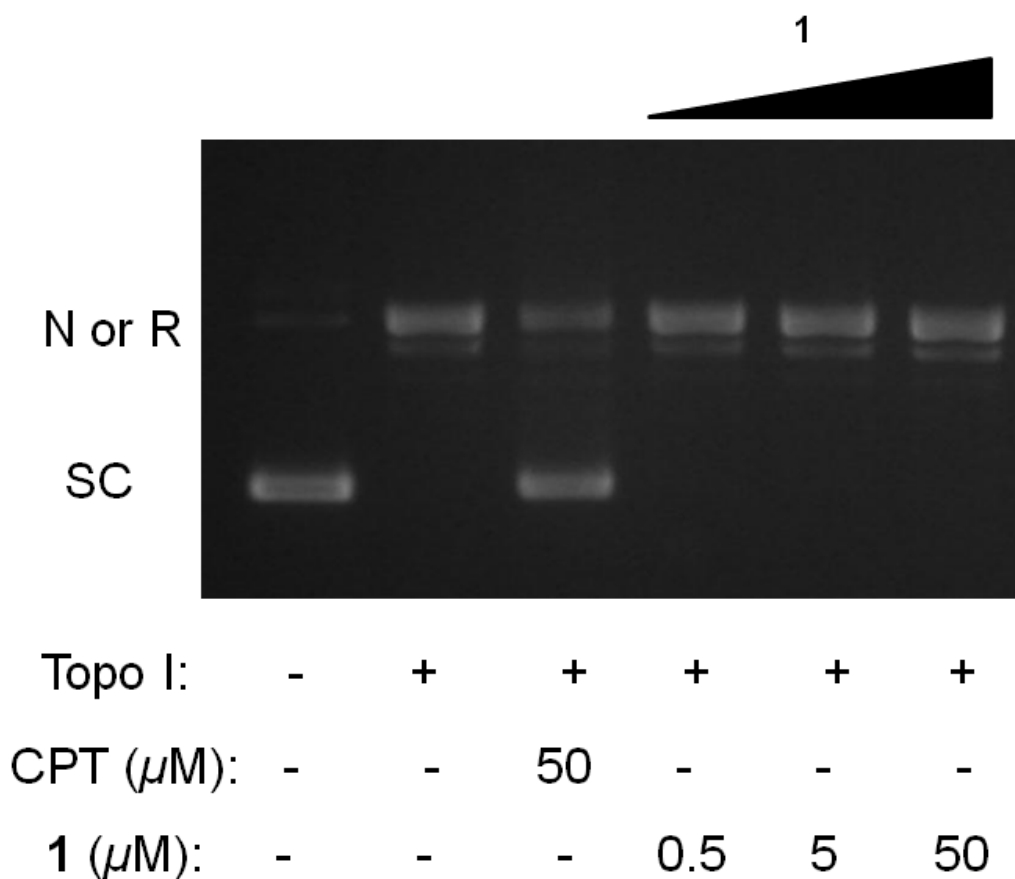


Figure S6. Electrophoresis on agarose gel comparing the effect of CPT and **1** on the relaxation plasmid DNA by human topoisomerase 1. N or R: nicked- or relaxed-form DNA; SC: supercoiled DNA.

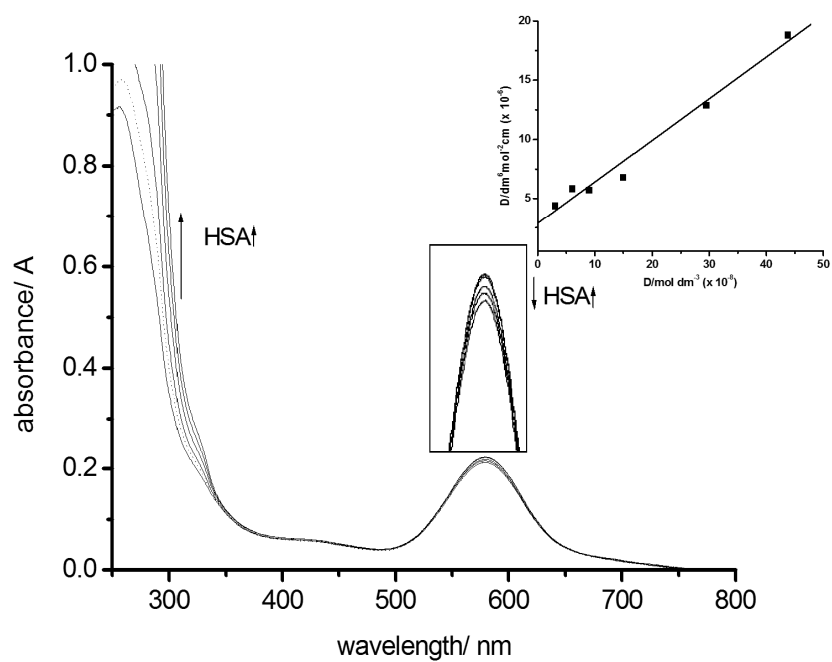


Figure S7. UV/Vis spectral changes of **1** a PBS-EtOH solution (19:1, v/v) with increasing concentration of human serum albumin (HSA).

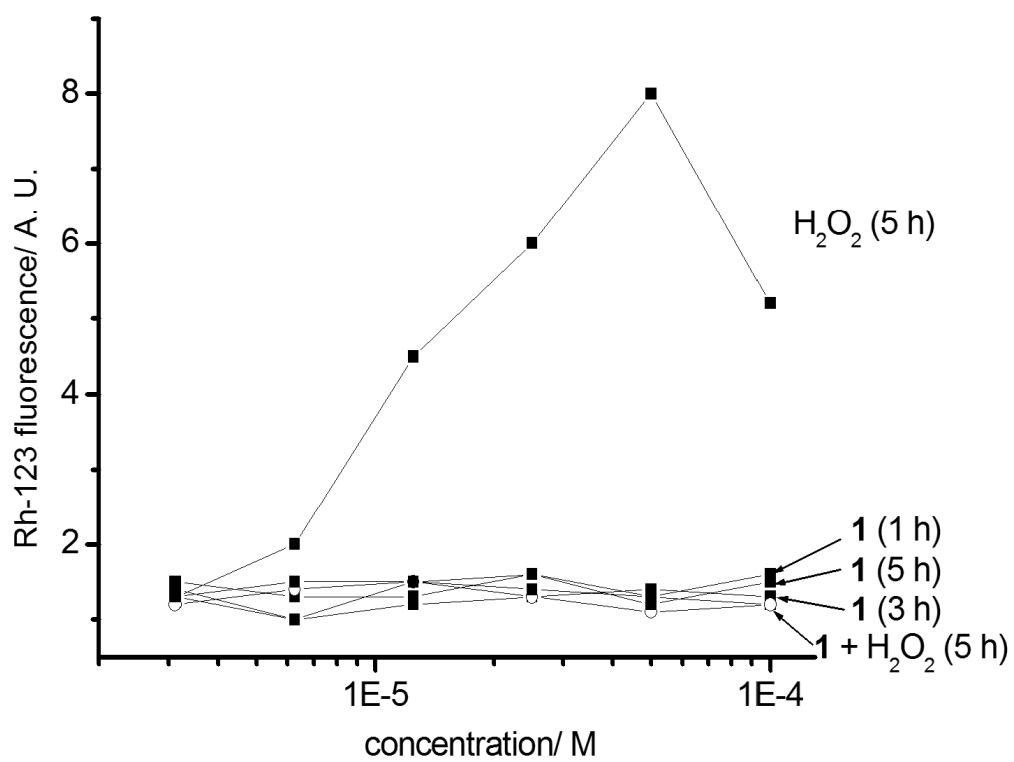


Figure S8. Detection of ROS generated in the untreated and **1**-treated HeLa cells.

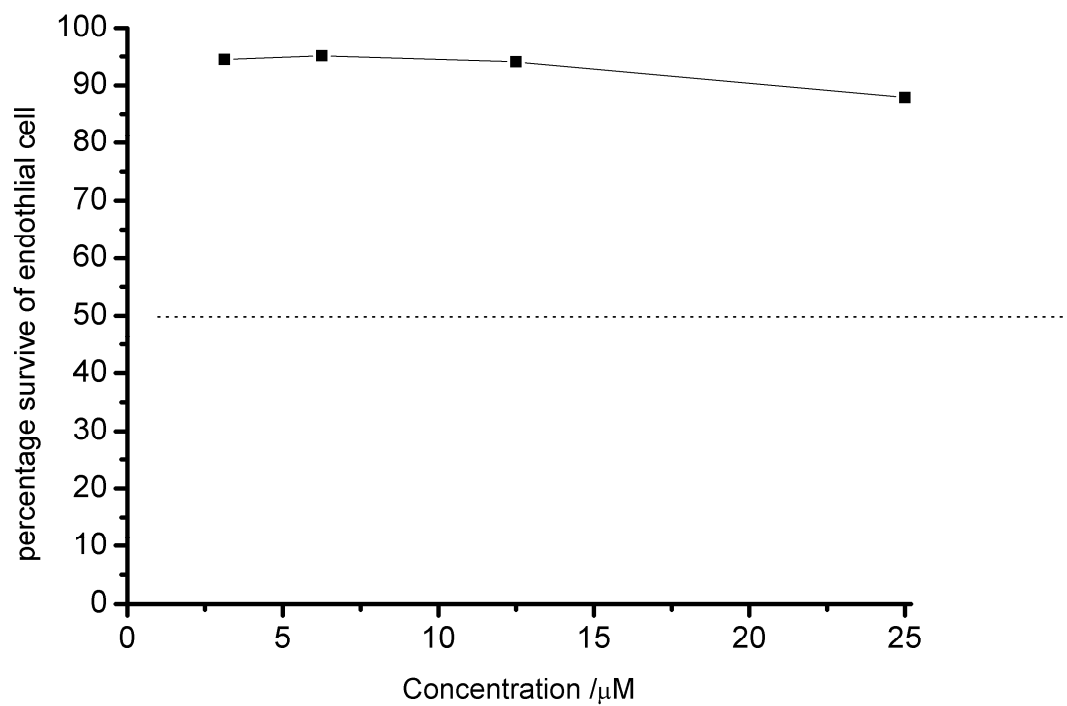


Figure S9. Cytotoxicity of **1** toward MS1 cells for 8 h.

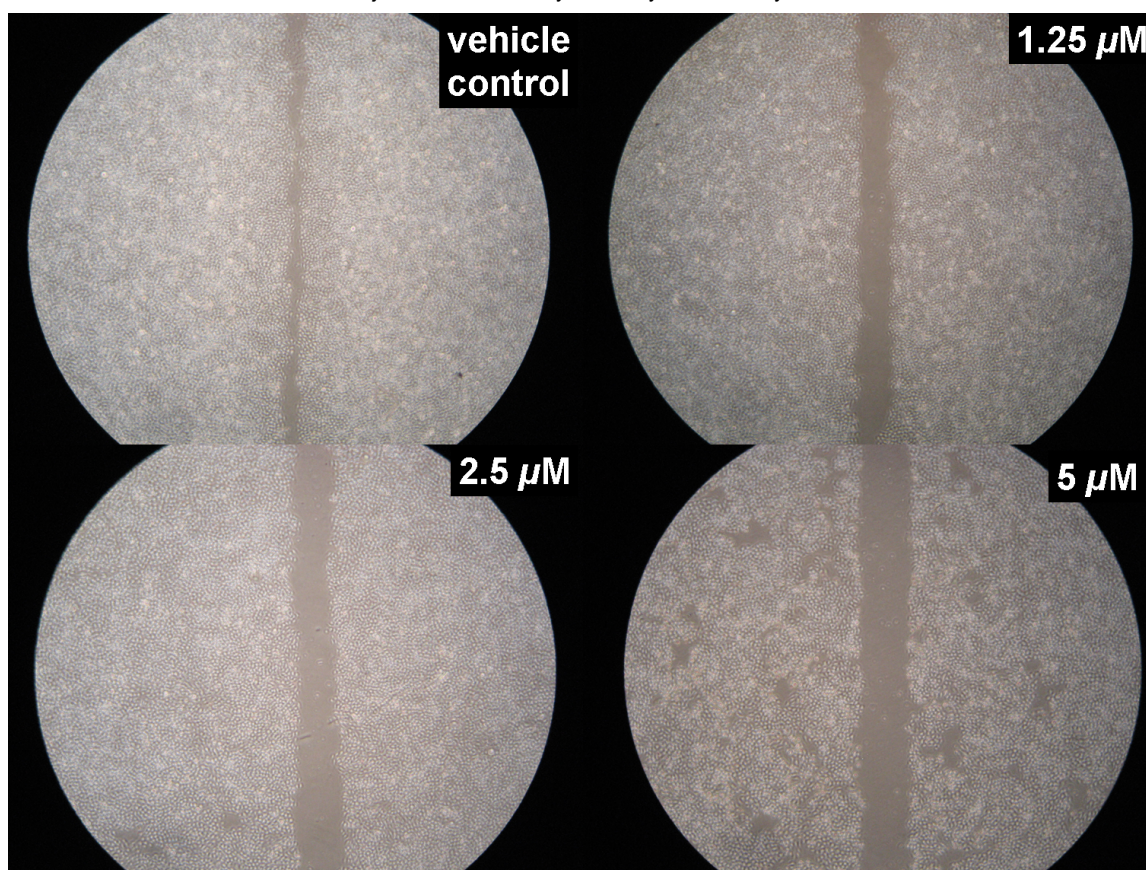


Figure S10. Dose-dependent inhibition of the migration of MS1 cells by **1**.

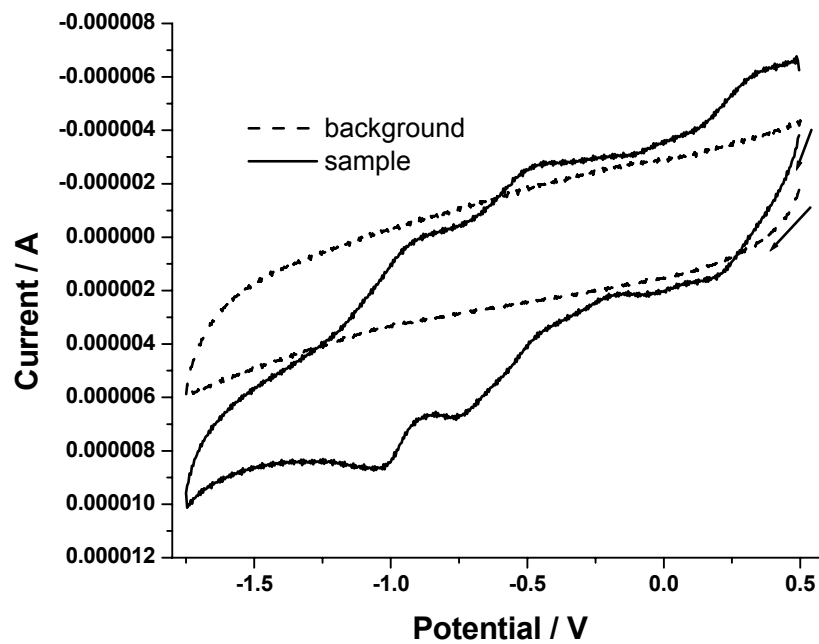


Figure S11. Cyclic voltammogram of **1** recorded in CH_2Cl_2 (0.1 M Bu_4NPF_6). Working electrode = glassy carbon, counter-electrode = platinum wire, reference electrode = Ag/AgNO_3 (0.1 M in CH_2Cl_2), scan rate = 100 mVs^{-1} .

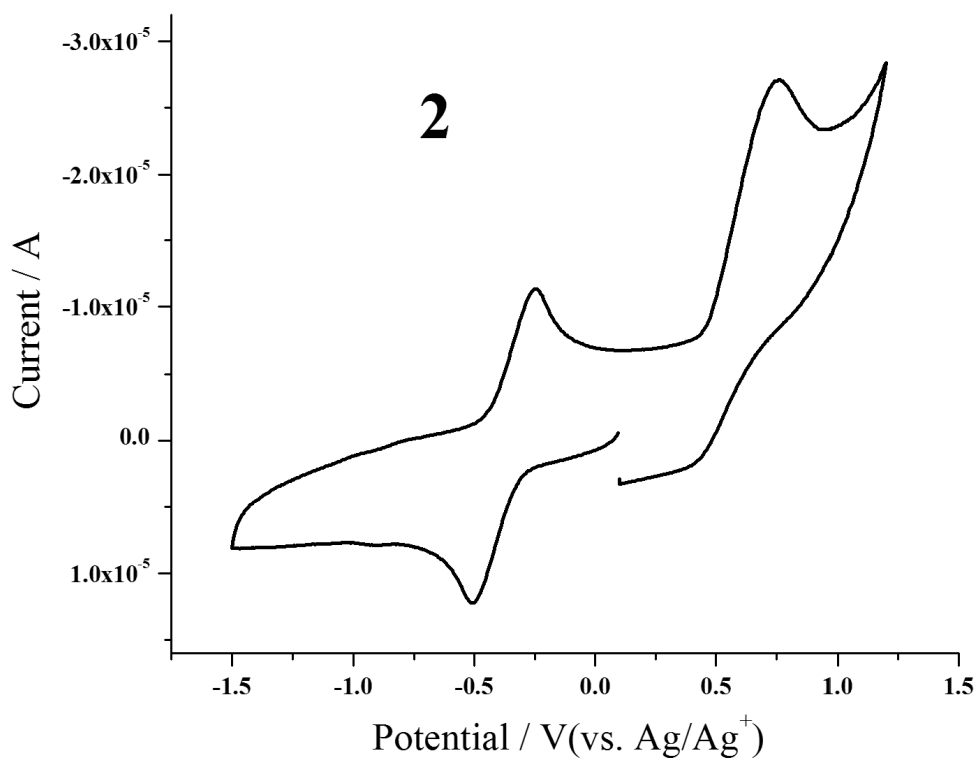


Figure S12. Cyclic voltammogram of **2** recorded in DMF (0.1 M Bu₄NPF₆). Working electrode = glassy carbon, counter-electrode = platinum wire, reference electrode = Ag/AgNO₃ (0.1 M in DMF), scan rate = 100 mVs⁻¹.

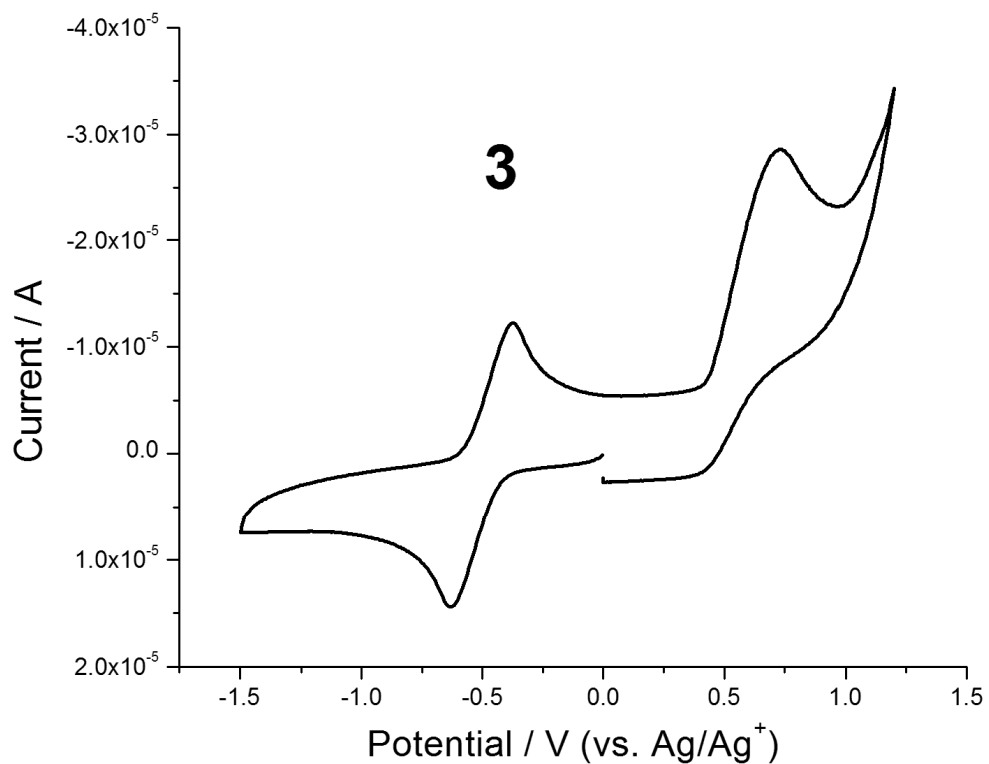


Figure S13. Cyclic voltammogram of **3** recorded in DMF (0.1 M Bu_4NPF_6). Working electrode = glassy carbon, counter-electrode = platinum wire, reference electrode = Ag/AgNO_3 (0.1 M in DMF), scan rate = 100 mVs^{-1} .

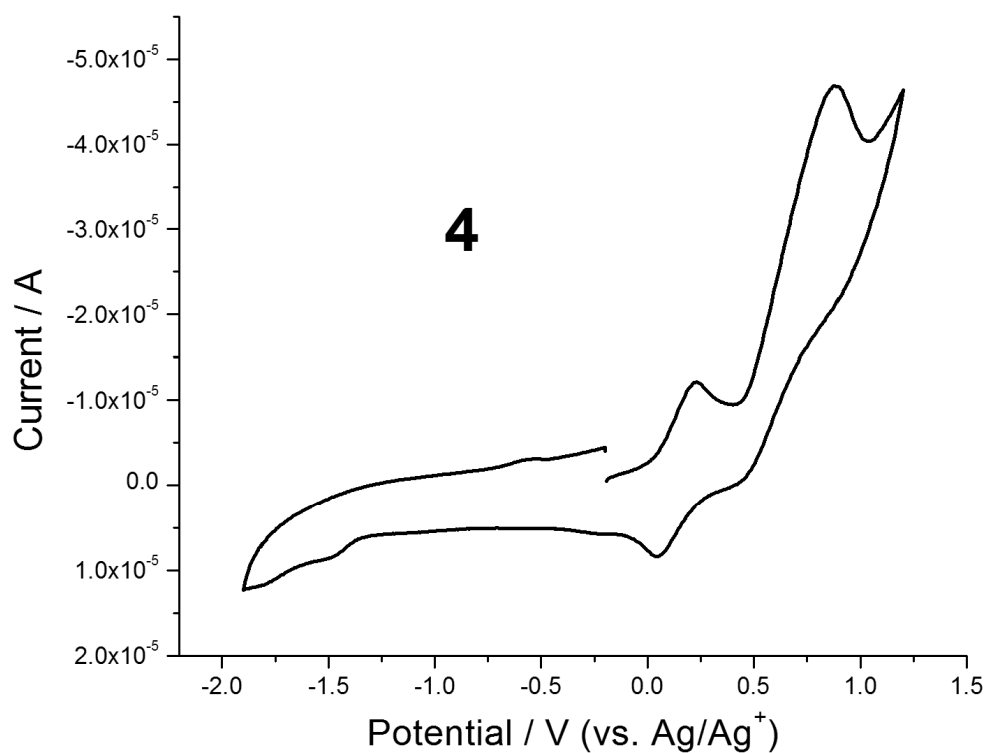


Figure S14. Cyclic voltammogram of **4** recorded in DMF (0.1 M Bu₄NPF₆). Working electrode = glassy carbon, counter-electrode = platinum wire, reference electrode = Ag/AgNO₃ (0.1 M in DMF), scan rate = 100 mVs⁻¹.

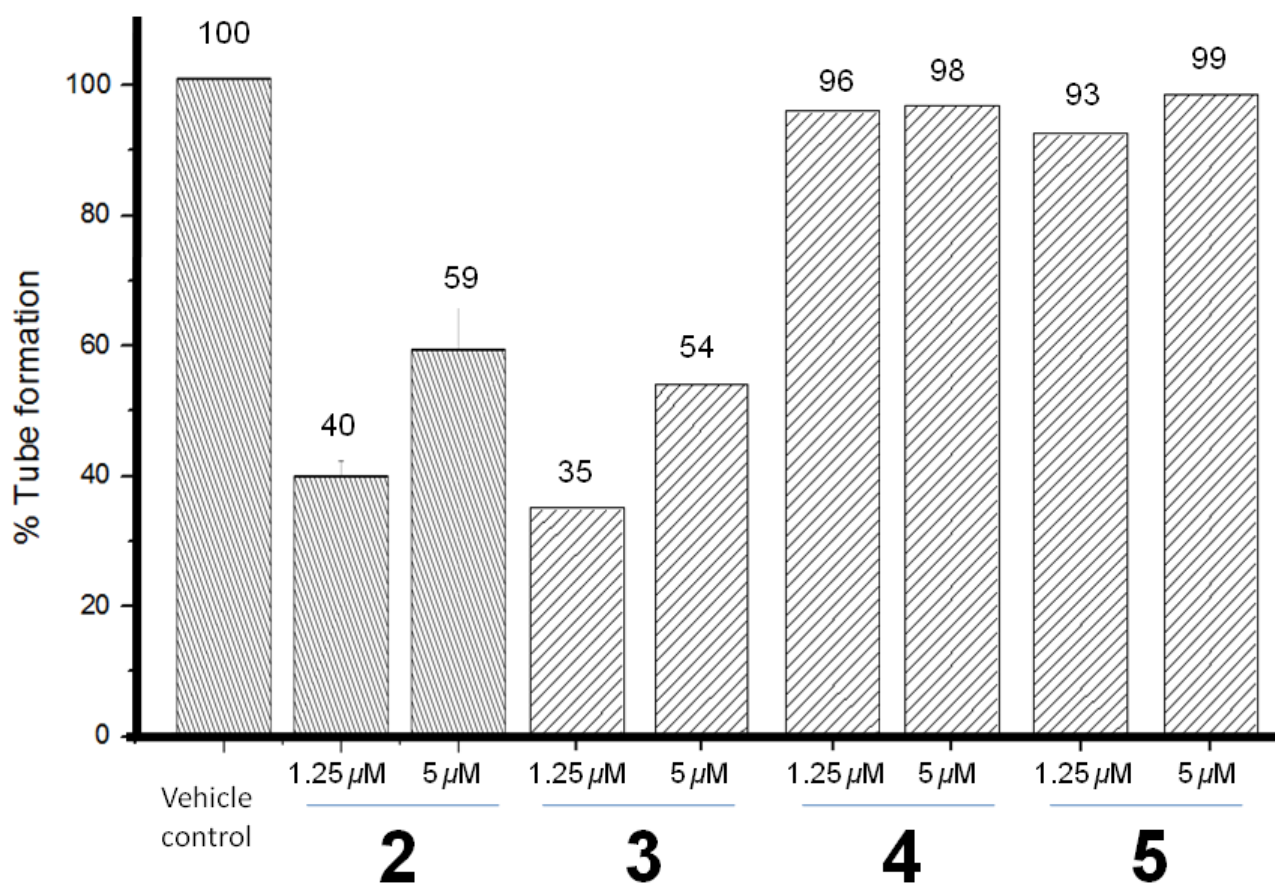


Figure S15. Inhibition of tube formation by 2, 3, 4 and 5 at 1.25 and 5 μM levels.

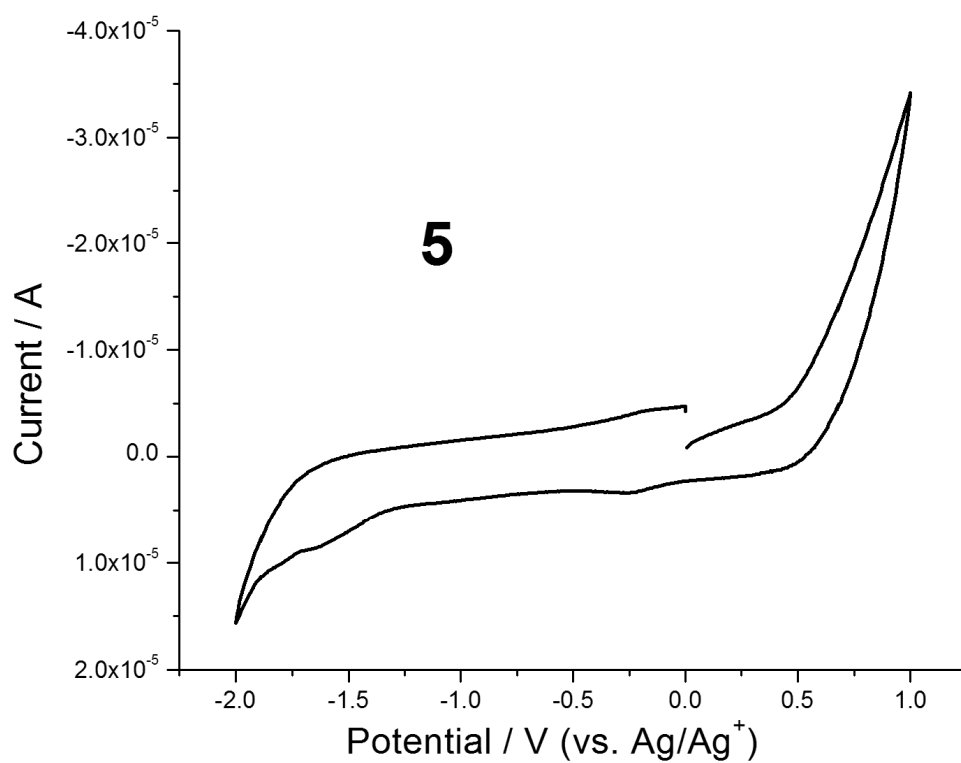


Figure S16. Cyclic voltammogram of **5** recorded in DMF (0.1 M Bu_4NPF_6). Working electrode = glassy carbon, counter-electrode = platinum wire, reference electrode = Ag/AgNO_3 (0.1 M in DMF), scan rate = 100 mVs^{-1} .

Table S1. Bond lengths [Å] and angles [°] for **1**.

Ru(1)-O(1)	1.902(5)
Ru(1)-N(2A)	2.038(5)
Ru(1)-N(1A)	2.064(5)
Ru(1)-N(5A)	2.083(5)
Ru(1)-N(3A)	2.092(5)
Ru(1)-N(4A)	2.105(6)
Ru(2)-O(1)	1.887(5)
Ru(2)-N(1B)	2.045(6)
Ru(2)-N(2B)	2.064(6)
Ru(2)-N(6A)	2.077(5)
Ru(2)-N(8A)	2.104(5)
Ru(2)-N(7A)	2.108(6)
N(1A)-C(11)	1.330(8)
N(1A)-N(1B)	1.366(8)
N(1B)-C(13)	1.352(9)
N(2A)-C(21)	1.341(8)
N(2A)-N(2B)	1.370(8)
N(2B)-C(23)	1.337(8)
N(3A)-C(31)	1.323(8)
N(3A)-N(3B)	1.372(8)
N(3B)-C(33)	1.342(8)
N(4A)-C(41)	1.330(9)
N(4A)-N(4B)	1.402(9)
N(4B)-C(43)	1.346(9)
N(5A)-C(51)	1.326(8)
N(5A)-N(5B)	1.364(8)
N(5B)-C(53)	1.329(8)
N(6A)-N(6B)	1.347(8)
N(6A)-C(61)	1.349(8)
N(6B)-C(63)	1.330(9)
N(7A)-C(71)	1.336(10)
N(7A)-N(7B)	1.359(8)
N(7B)-C(73)	1.318(10)
N(8A)-N(8B)	1.325(8)
N(8A)-C(81)	1.345(8)
N(8B)-C(83)	1.340(9)
C(11)-C(12)	1.403(9)

C(12)-C(13)	1.378(10)
C(21)-C(22)	1.382(9)
C(22)-C(23)	1.381(9)
C(31)-C(32)	1.387(9)
C(32)-C(33)	1.388(10)
C(41)-C(42)	1.393(11)
C(42)-C(43)	1.366(11)
C(51)-C(52)	1.404(9)
C(52)-C(53)	1.364(9)
C(61)-C(62)	1.379(9)
C(62)-C(63)	1.388(10)
C(71)-C(72)	1.374(11)
C(72)-C(73)	1.392(11)
C(81)-C(82)	1.393(9)
C(82)-C(83)	1.360(10)

O(1)-Ru(1)-N(2A)	86.38(19)
O(1)-Ru(1)-N(1A)	86.75(18)
N(2A)-Ru(1)-N(1A)	86.9(2)
O(1)-Ru(1)-N(5A)	87.87(19)
N(2A)-Ru(1)-N(5A)	90.4(2)
N(1A)-Ru(1)-N(5A)	174.1(2)
O(1)-Ru(1)-N(3A)	90.09(19)
N(2A)-Ru(1)-N(3A)	176.2(2)
N(1A)-Ru(1)-N(3A)	91.6(2)
N(5A)-Ru(1)-N(3A)	90.7(2)
O(1)-Ru(1)-N(4A)	178.22(17)
N(2A)-Ru(1)-N(4A)	92.0(2)
N(1A)-Ru(1)-N(4A)	94.0(2)
N(5A)-Ru(1)-N(4A)	91.3(2)
N(3A)-Ru(1)-N(4A)	91.5(2)
O(1)-Ru(2)-N(1B)	85.6(2)
O(1)-Ru(2)-N(2B)	86.0(2)
N(1B)-Ru(2)-N(2B)	88.6(3)
O(1)-Ru(2)-N(6A)	93.05(19)
N(1B)-Ru(2)-N(6A)	89.5(2)
N(2B)-Ru(2)-N(6A)	177.9(2)
O(1)-Ru(2)-N(8A)	92.63(19)
N(1B)-Ru(2)-N(8A)	177.5(2)
N(2B)-Ru(2)-N(8A)	89.6(2)

N(6A)-Ru(2)-N(8A)	92.3(2)
O(1)-Ru(2)-N(7A)	175.1(2)
N(1B)-Ru(2)-N(7A)	90.1(2)
N(2B)-Ru(2)-N(7A)	91.5(2)
N(6A)-Ru(2)-N(7A)	89.3(2)
N(8A)-Ru(2)-N(7A)	91.5(2)
Ru(2)-O(1)-Ru(1)	114.6(3)
C(11)-N(1A)-N(1B)	108.6(5)
C(11)-N(1A)-Ru(1)	136.6(4)
N(1B)-N(1A)-Ru(1)	114.7(4)
C(13)-N(1B)-N(1A)	108.0(5)
C(13)-N(1B)-Ru(2)	134.1(5)
N(1A)-N(1B)-Ru(2)	117.9(4)
C(21)-N(2A)-N(2B)	107.3(5)
C(21)-N(2A)-Ru(1)	135.6(4)
N(2B)-N(2A)-Ru(1)	117.0(4)
C(23)-N(2B)-N(2A)	108.3(5)
C(23)-N(2B)-Ru(2)	136.0(5)
N(2A)-N(2B)-Ru(2)	115.6(4)
C(31)-N(3A)-N(3B)	104.7(5)
C(31)-N(3A)-Ru(1)	130.4(4)
N(3B)-N(3A)-Ru(1)	125.0(4)
C(33)-N(3B)-N(3A)	111.4(5)
C(41)-N(4A)-N(4B)	109.3(6)
C(41)-N(4A)-Ru(1)	128.6(6)
N(4B)-N(4A)-Ru(1)	122.1(4)
C(43)-N(4B)-N(4A)	105.2(6)
C(51)-N(5A)-N(5B)	105.2(5)
C(51)-N(5A)-Ru(1)	130.1(4)
N(5B)-N(5A)-Ru(1)	124.7(4)
C(53)-N(5B)-N(5A)	110.7(5)
N(6B)-N(6A)-C(61)	108.5(5)
N(6B)-N(6A)-Ru(2)	124.2(4)
C(61)-N(6A)-Ru(2)	127.3(4)
C(63)-N(6B)-N(6A)	107.7(6)
C(71)-N(7A)-N(7B)	105.2(6)
C(71)-N(7A)-Ru(2)	135.0(5)
N(7B)-N(7A)-Ru(2)	119.8(5)
C(73)-N(7B)-N(7A)	111.7(6)
N(8B)-N(8A)-C(81)	106.7(5)

N(8B)-N(8A)-Ru(2)	124.2(4)
C(81)-N(8A)-Ru(2)	129.0(4)
N(8A)-N(8B)-C(83)	110.4(6)
N(1A)-C(11)-C(12)	109.1(6)
C(13)-C(12)-C(11)	105.1(6)
N(1B)-C(13)-C(12)	109.2(6)
N(2A)-C(21)-C(22)	110.0(5)
C(23)-C(22)-C(21)	104.8(6)
N(2B)-C(23)-C(22)	109.6(6)
N(3A)-C(31)-C(32)	112.2(6)
C(31)-C(32)-C(33)	104.8(6)
N(3B)-C(33)-C(32)	107.0(6)
N(4A)-C(41)-C(42)	108.7(7)
C(43)-C(42)-C(41)	105.4(7)
N(4B)-C(43)-C(42)	111.3(7)
N(5A)-C(51)-C(52)	111.3(5)
C(53)-C(52)-C(51)	103.9(5)
N(5B)-C(53)-C(52)	108.9(6)
N(6A)-C(61)-C(62)	109.3(6)
C(61)-C(62)-C(63)	103.9(6)
N(6B)-C(63)-C(62)	110.6(6)
N(7A)-C(71)-C(72)	110.9(7)
C(71)-C(72)-C(73)	105.1(7)
N(7B)-C(73)-C(72)	107.2(6)
N(8A)-C(81)-C(82)	109.6(6)
C(83)-C(82)-C(81)	104.6(6)
N(8B)-C(83)-C(82)	108.7(6)